Comparison of strain localization properties of dense clean sand and well-graded gravel in plane strain compression tests

Comparaison de la localisation des déformations au cours d'essais de déformations planes sur un sable dense et sur un gravier compacté

Y. Tsutsumi
Institute of Industrial Science, The University of Tokyo, Tokyo, Japan
S. Maqbool
University of Engineering and Technology, Lahore, Pakistan

ABSTRACT
To investigate the effects of confining stress, particle size and uniformity coefficient on local deformation characteristics of granular materials, strain localization properties of a dense clean sand under different confining stresses up to 2400 kPa and those of a compacted well-graded gravel having large particles were compared in drained plane strain compression tests. Newly developed medium-pressure plane strain compression test apparatus and large-scale plane strain compression test apparatus were employed for testing the sand and gravel, respectively, and a fully-automated image analysis technique was introduced to evaluate their local deformation properties including strain localization. Discussions were made by focusing on stress-strain relationships, strain localization properties until peak stress state, clarity and thickness of shear bands observed at the end of the tests, and orientation of shear bands in relation to directions of maximum stress obliquity and zero extension.

RÉSUMÉ
Les influences de la pression de confinement, de la taille des grains et de leur uniformité sur la localisation des déformations au sein de milieux granulaires ont été évaluées à partir d'essais de déformation plane réalisés sur un sable fin uniforme et sur un gravier compacté à granulométrie étalée. Les pressions de confinement maximales appliquées atteignent 2400 kPa. Un large appareil biaxial a été utilisé dans le cas du gravier compacté tandis qu'un nouvel appareil biaxial récemment développé, de dimensions plus réduites, a été employé dans le cas du sable fin uniforme. Les champs de déformation ont été obtenus par analyse photogrammétrique. Les courbes de contrainte-déformation, la localisation des déformations avant rupture, la clarté et l'épaisseur des bandes de cisaillement observées à la fin des essais ainsi que leur orientation sont précisèment discutées.

Keywords : plane strain compression test, image analysis, strain localization, shear band

1 INTRODUCTION

It is well known that dense granular materials and geomaterials having cementation on their micromechanical structure exhibit strain softening behavior which is associated with strain localization or formation of shear band. Recently, performance based designs have been adopted into aseismic design of earth structures and large foundations on subsoil layers composed of these materials. As one of the attempts, for example, strain localization properties of several granular materials were investigated by using plane strain compression (herein denoted as PSC) tests and taken into account in evaluating displacements of earth structures that are subjected to seismic load by modified Newmark method along the critical failure plane (e.g., Yoshida & Tatsuoka 1997, Okuyama et al. 2003). In such past studies, however, the gradation range of materials tested, the levels of confining stress employed, and the accuracies in evaluation of strain localization were limited due to the capacities of test apparatuses and image processing techniques.

To investigate the effects of confining stress, particle size and uniformity coefficient on local deformation characteristics of granular materials, therefore, strain localization properties of a dense clean sand under different confining stresses up to 2400 kPa and those of a compacted well-graded gravel having large particles were compared in drained PSC tests. Newly developed medium-pressure PSC test apparatus and large-scale PSC test apparatus were employed for testing the sand and gravel, respectively, and a fully-automated image analysis technique was introduced to evaluate their local deformation properties including strain localization.

2 MATERIALS, EQUIPMENTS AND PROCEDURES OF TESTS AND IMAGE ANALYSES

Toyoura sand as a clean and fine sand and a well-graded gravel called Chiba gravel were employed as the test materials. Their mean grain size D_{50}, maximum grain size D_{max}, uniformity coefficient Uc and soil particle density Gs and those of sand and gravel materials studied by Yoshida & Tatsuoka (1997) and Okuyama et al. (2003) are summarized in Table 1.

Table 1. Physical properties of materials tested in this study and by Yoshida & Tatsuoka (1997) and Okuyama et al. (2003)

Material	D_{50} (mm)	D_{max} (mm)	Uc	Gs
Toyoura sand	0.205	-	1.59	2.656
Chiba gravel	11	38	30	-
Poorly graded sand*	0.174 - 0.681	-	1.20 - 2.13	2.49 - 2.72
Poorly graded gravel*	1.62 - 2.01	-	1.36 - 1.46	2.65 - 2.67
Well graded sand**	0.66 - 0.68	-	6.45 - 7.8	2.69 - 2.89
Well graded gravel**	2.49	4.75	4.1	-

* Materials studied by Yoshida & Tatsuoka (1997)
** Materials studied by Okuyama et al. (2003)

A medium-pressure PSC test apparatus (Tsutsumi et al. 2008) was used for testing Toyoura sand. To measure global volumetric strain during testing based on the volume of drained water from a specimen, a low capacity differential pressure transducer was employed. Prismatic specimens with the dimensions shown schematically in Figure 1 a) were prepared by air pluviation technique. After applying the confining stress, or the effective minor principal stress σ_3', of 30 kPa by partial vacuum, a pair of confining plates was fixed to apply an initial deviator stress q_2 (= σ_2 - σ_3) of about 30 kPa in the horizontal direction perpendicular to the confining plates. After saturation,

Proceedings of the 17th International Conference on Soil Mechanics and Geotechnical Engineering
M. Hamza et al. (Eds.)

doi:10.3233/978-1-60750-031-5-388

specimens were subjected to anisotropic consolidation under different levels of confining stress. The value of the effective principal stress ratio σ_1'/σ_3' at the end of the anisotropic consolidation was set around 2.2, while keeping the value of q_2 to be positive. Dry densities of the specimens after the anisotropic consolidation ρ_{d0} were within the range of 1.595 to 1.621 g/cm^3. Under the confining stresses of 50, 200, 400, 800, 1600, and 2400 kPa, they were subjected to drained monotonic vertical loading at an axial strain rate of 0.05 %/min.

A large-scale PSC test apparatus (Tsutsumi et al. 2006) was used for Chiba gravel. Transducers to measure the value of minor principal strain ε_3 called hereafter as CLDTs were set at two different heights as schematically shown in Fig. 1 b). A prismatic specimen with the dimensions shown in Fig. 1 b) was prepared at an initial water content of 5.5 % by employing heavy dynamic compaction using an automatic compactor to achieve the initial dry density ρ_{di} of 1.95 g/cm^3. Under partially saturated condition, the specimen was consolidated isotropically to a confining stress of 78 kPa by increasing the partial vacuum applied as the back pressure. After fixing a pair of confining plates and applying an initial horizontal deviator stress q_2 of 6 kPa, the specimen was subjected to monotonic vertical loading at an axial strain rate of 0.08 %/min.

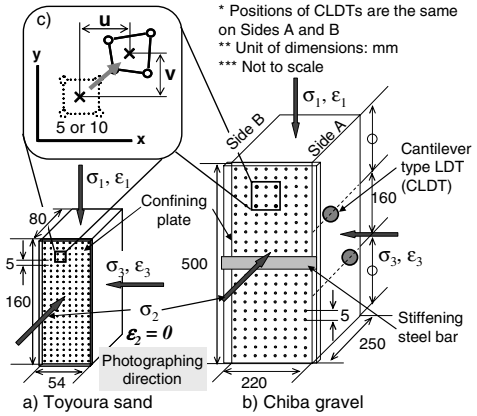

Figure 1. Dimensions of specimens, positions of transducers and definition of element for image analysis

Digital photographs (3264 x 2448 pixels) of the specimen's side surface were taken through transparent planner windows of the confining plate and the pressure cell during anisotropic consolidation and monotonic loading on Toyoura sand. During monotonic loading on Chiba gravel, digital photographs were taken through the transparent confining plate having a stiffening steel bar at the central height. These photographs were taken at a constant time interval during the stages of anisotropic consolidation, and at a constant major principal strain increments during monotonic loading. On the observed surface of the membrane that covered the specimen, a series of equally spaced points made of rubber had been imprinted at a spacing of 5 mm. The displacements of each point were read from the photographs, which were used for the computation of local strains, i.e., the major and minor principal strains ε_1 and ε_3 of each element consisting of four grid nodes at a spacing of 5 mm on Toyoura sand and 10 mm on Chiba gravel. As shown in Fig. 1 c), the horizontal and vertical displacements at the center of the element, u and v were converted to ε_1 and ε_3.

3 TEST RESULTS AND DISCUSSIONS

3.1 *Comparison of stress-strain relationships*

Typical relationships between the principal stress ratio R= σ_1'/σ_3', the global volumetric strain ε_{vol_LCDPT} and the major principal strain measured by external transducer ε_{1_EXT} under the different levels of σ_3' in drained monotonic loading on Toyoura sand are compared in Figure 2. In Fig. 2 b), the initial values of ε_{vol} (denoted as ε_{vol0}) are indicated as the volume change during anisotoropic consolidation. Before the peak stress state, the values of R that were mobilized at the same value of ε_{1_EXT} decreased with the increase in σ_3' as shown in Fig. 2 a). The peak stress ratios R_{max} under σ_3' of 50, 200 and 400 kPa were almost similar to each other while the amounts of ε_{1_EXT} at R_{max} increased with the increase in σ_3'. On the other hand, the values of R_{max} under the σ_3' values exceeding 800 kPa decreased with the increase in σ_3', while the values of ε_{1_EXT} at R_{max} were almost the same as the one that was obtained under σ_3' of 400 kPa.

After the peak stress state, strain softening behavior and formation of clear single shear band were identified in all the tests as shown later. The values of R at residual stress state were distributed within a rather narrow range, from about 3.2 to 4.5, irrespective of the significant difference in the value of R_{max}.

As shown in Fig. 2 b), the value of ε_{vol0} was naturally larger under higher level of σ_3'. Besides, considerably less dilative behavior during monotonic loading was observed under the σ_3' values exceeding 800 kPa. This trend would be linked with the decrease in the value of R_{max} as explained above.

According to the results of the measurements by transducers and image analyses during anisotropic consolidation, more contractive and uniform deformation was observed under higher confining stress. These would have resulted in the increase in the values of ε_{1_EXT} at peak stress state under σ_3' of less than 400 kPa. On the other hand, slight increase in the fines content could be recognized from the gradation curves of the material after the tests under higher confining stress. Consequently, particle crushing would have caused the decrease in peak principal stress ratios under σ_3' of more than 800 kPa (Tsutsumi et al 2008).

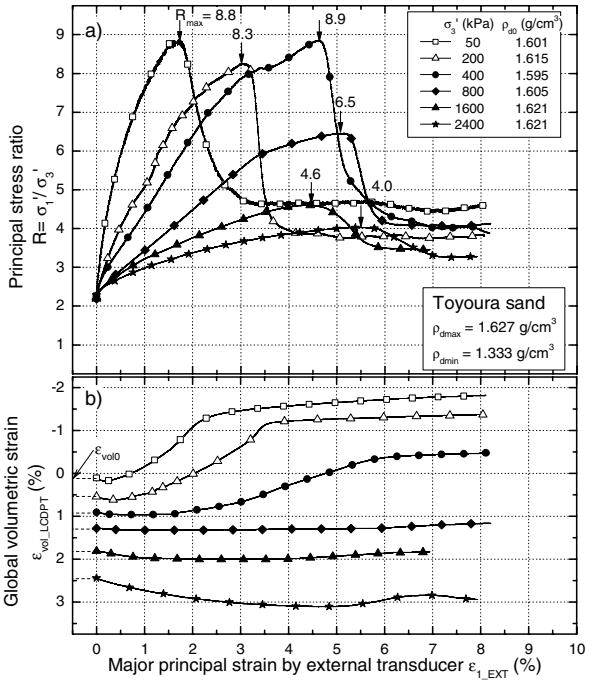

Figure 2. Typical stress-strain relationships of Toyoura sand

Relationships between the accumulation of R, ε_{vol} and ε_{1_EXT} during drained monotonic loading on Chiba gravel are shown in Figure 3. In Fig. 3 b), the value of ε_{vol} is set to be zero in the beginning of monotonic loading and evaluated by summation of the normal strain measurements by the CLDTs and the external transducer, while neglecting intermediate principal strain ε_2 which is actually a non-zero value due to the effects of bedding error at the interfere between the specimen and the confining plate (Maqbool et al. 2003). The value of R gradually increased

up to peak stress state after the rapid increase in R in the beginning of loading. In contrast to the relationships after peak stress state on Toyoura sand, reduction of R was not significant and dilative behavior was observed until the end of loading, although formation of single shear band could be identified by visual inspection of the specimen after the test.

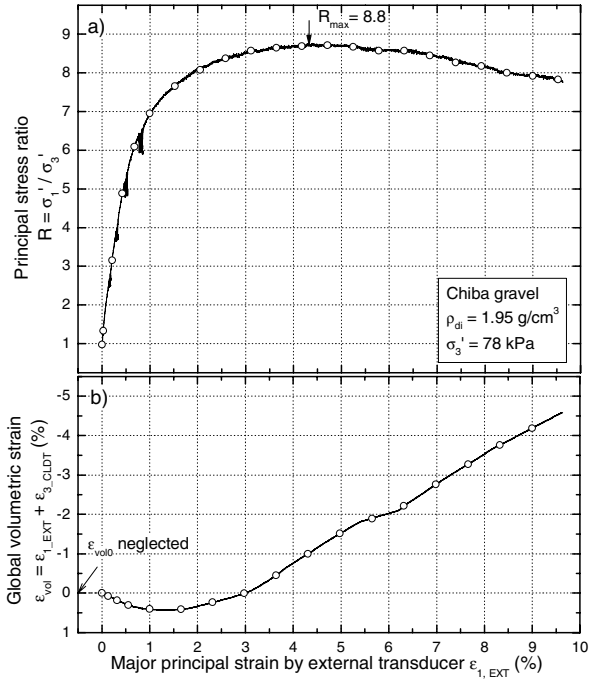

Figure 3. Stress-strain relationship of Chiba gravel

3.2 *Comparison of strain localization characteristics until peak stress state*

Distributions of the maximum shear strain increment $\Delta\gamma_{max}$ (= $\Delta\varepsilon_1$ - $\Delta\varepsilon_3$) at the values of R equal to a) 4.0, b) 6.0, c) 8.0, d) R_{max} and e) just after peak stress state on Toyoura sand under σ_3' of 400 kPa, and on Chiba gravel are shown in Figures 4 and 5, respectively.

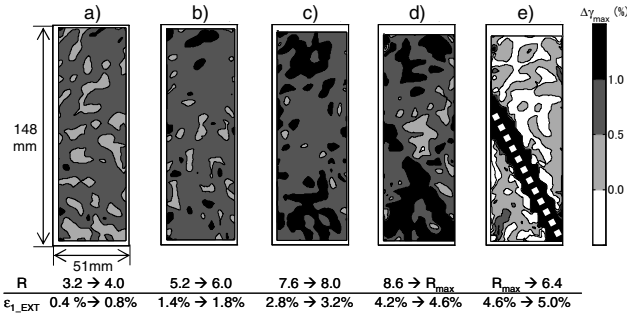

Figure 4. Distributions of the maximum shear strain increment on Toyoura sand (σ_3' = 400 kPa)

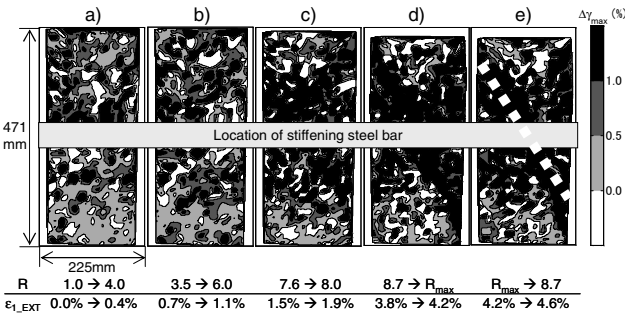

Figure 5. Distributions of the maximum shear strain increment on Chiba gravel (σ_3' = 78 kPa)

As the value of R_{max} was almost the same with the test result on Chiba gravel while including similar values of ε_{1_EXT} at the peak stress state, the test result on Toyoura sand under σ_3' of 400 kPa is hereafter selected as their representative. White dotted lines in Figs. 4 and 5 indicate the locations of final shear band. In Fig. 5, the central height region is not analyzed due to the existence of the stiffening steel bar.

In both of the tests, several strain localization zones could be distinguished in the $\Delta\gamma_{max}$ distributions until the peak stress state as shown in Figs. 4 and 5 a) - d). After that, in the test on Toyoura sand, large accumulations of γ_{max} concentrated on one of them where a full shear band was formed as shown in Fig. 4 e). On the other hand, in the test on Chiba gravel, the strain accumulated not only at the location of the final shear band but also at the other zones where significant strain localization was observed before the peak stress state as shown in Fig. 5 e). It can be inferred that such different tendencies after peak stress state caused the difference in the degree of post-peak reduction in R values as mentioned before (see Figs. 2 a) and 3 a)).

3.3 *Characteristics of shear band observed at the end of loading*

Figure 6 shows a) distribution of $\Delta\gamma_{max}$ during post-peak reduction (from R = R_{max} to 4.0), b) observed surface of the specimen at ε_{1_EXT} of 8.0 % and c) magnified view of the area indicated in b) with dotted rectangle on Toyoura sand under σ_3' of 400 kPa (i.e., the same test as shown in Fig. 4). Location of a band connecting areas with the value of $\Delta\gamma_{max}$ more than 60 % in Fig. 6 a) coincided with the location of shear band shown in Figs. 6 b) and c). Based on visual inspection of the photograph shown in Fig. 6 c), the thickness of the shear band of Toyoura sand is approximately 2 - 3 mm. The other regions mostly underwent negative increment in the values of $\Delta\gamma_{max}$.

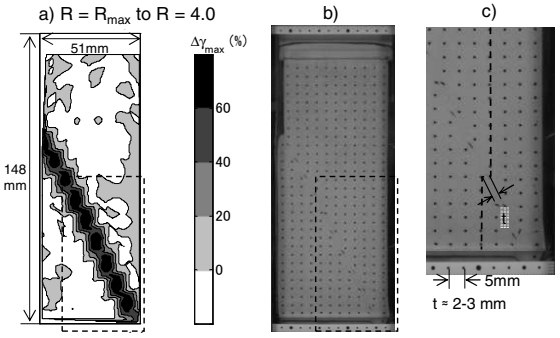

Figure 6. Observation of shear band on Toyoura sand (σ_3' = 400 kPa)

Figure 7 shows the same sets of data on Chiba gravel. As residual stress state was not clearly observed in this test, Fig. 7 a) shows distribution of $\Delta\gamma_{max}$ after peak stress state until the end of the test (from R = R_{max} to 7.8). The largest increase in the values of $\Delta\gamma_{max}$ could be recognized at the location of the shear band that was observed visually, while the values of $\Delta\gamma_{max}$ increased as well over the whole regions of the specimen. As the clarity of the zone of shear band in Fig. 7 c) was not enough to identify its thickness, imprinted points on the membrane were connected in vertical direction and the locations of two points having the largest curvature of the line was used to evaluate the shear band thickness, t, as shown in the figure. The t value was of the order of centimeters and found to be much larger than that of Toyoura sand.

On Toyoura sand, i.e. poorly graded and fine sand, strain localization to the shear band with small thickness after peak stress state caused the rapid and drastic decrease of its mobilized strength to residual state. On the other hand, the mobilized strength of Chiba gravel, well-graded gravelly soil, did not change largely after the peak stress state. It was caused by lesser extent of strain localization and formation of less clear and much thicker shear band as compare to Toyoura sand.

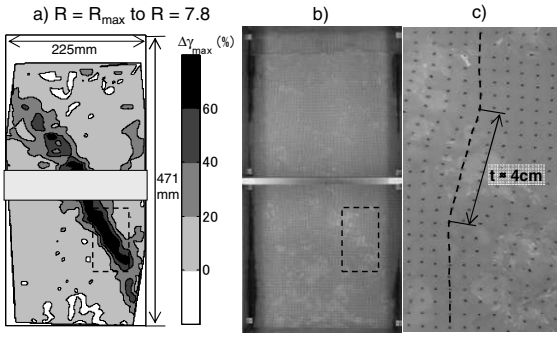

Figure 7. Observation of shear band on Chiba gravel (σ_3' = 78 kPa)

3.4 *Direction of shear band in plane strain compression test*

According to the analyses of PSC tests on poorly graded sands and gravels conducted by Yoshida & Tatsuoka (1997), the orientation of shear band, θ, as defined in Figure 8 is found to be between the direction of maximum stress obliquity, $\theta_C = 45 + \phi_{0\_peak} / 2$ (deg.), and the direction of zero extension, $\theta_R = 45 + \upsilon_f / 2$ (deg). ϕ_{0_peak} and υ_f are mobilized angles of internal friction and dilatancy, respectively, at peak stress state defined by Equations (1) and (2). As the confining stress and/or the mean particle diameter of the tested materials increased, the values of θ and θ_R became closer to each other.

$$\phi_{0\_peak} = [\sin^{-1}\{(\sigma_1' - \sigma_3') / (\sigma_1' + \sigma_3')\}]_{\_peak} \quad (1)$$

$$\upsilon_f = [-\sin^{-1}\{(\Delta\varepsilon_1 + \Delta\varepsilon_3) / (\Delta\varepsilon_1 - \Delta\varepsilon_3)\}]_{\_peak} \quad (2)$$

The relationships between normalized shear band inclination and ratio of mean particle diameter, D_{50}, to specimen width, W, obtained by Yoshida & Tatsuoka (1997) are compared in Fig. 8 with the results on well graded sand and gravels by Okuyama et al. (2003), Toyoura sand and Chiba gravel in this study. On Toyoura sand, the value of θ was calculated from the coordinates of imprinted points included in the location of shear band by referring to Fig. 6 b). As mentioned in *3.2*, the region with the value of $\Delta\gamma_{max}$ during the post-peak stress reduction of more than 60 % corresponded to the full shear band in the case of Toyoura sand. By applying this result to Chiba gravel, the value of θ was evaluated from the inclination of linear fitting equation of the imprinted points within the region with the value of $\Delta\gamma_{max}$ of more than 60 % in Fig. 7 a).

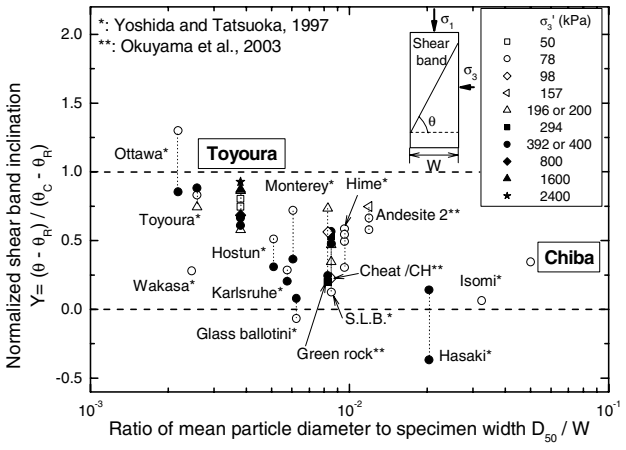

Figure 8. Orientation of shear band in plane strain compression tests on sand and gravel materials

In general, the trends of behavior obtained in the study by Okuyama et al. (2003) and in this study as shown in Fig. 8 agreed with those by Yoshida & Tatsuoka (1997). In other words, the directions of θ were found to be between the directions of θ_C and θ_R. As the value of D_{50}/W increased, the values of θ and θ_R became closer to each other, irrespective of the difference in the uniformity coefficient Uc as shown in Table 1. Furthermore, the θ values of Toyoura sand are closer to the θ_C values, irrespective of the different levels of σ_3', while the θ value of Chiba gravel having the largest value of D_{50}/W is closer to the θ_R value as are cases with the other gravelly soils.

4 CONCLUTIONS

As a result of the plane strain compression tests on dense Toyoura sand under the confining stresses over a range from 800 to 2400 kPa, the peak principal stress ratios decreased with the increase in the levels of the confining stress. On the other hand, when the confining stress was below 800 kPa, almost the same peak principal stress ratios were obtained. Strain softening behavior was observed clearly in all the tests on Toyoura sand, while no significant decrease in the mobilized strength of compacted Chiba gravel after the peak stress state was observed.

After the peak stress state, in the specimen of Toyoura sand, the local maximum shear strain concentrated on the zone where the shear band was formed fully. On the other hand, in the case of Chiba gravel, the local strain accumulated not only at the location of the full shear band but also at the other zones where significant strain localization was observed even before the peak stress state. In addition, the thickness of the shear band of Toyoura sand was approximately 2 - 3 mm, while that of Chiba gravel was much larger. It was inferred that the above differences in the post-peak behavior of these materials are affected by their different strain localization properties.

The results of plane strain compression tests on several kinds of sands and gravels conducted in this study and previous relevant studies were analyzed, and the orientations of shear bands were found to be between the directions of maximum stress obliquity and zero extension. Additionally, as the ratio of the mean particle diameter to specimen width increased, the orientation of the shear band and the direction of zero extension became closer to each other, irrespective of the difference in the values of their uniformity coefficient.

REFERENCES

Maqbool, S., Sato, T. & Koseki, J. 2003. Comparison of plane strain compression tests using active and passive controls with triaxial compression tests on gravel. *Proceedings of 5th International Summer Symposium, International Activities Committee, JSCE*: 229-232

Okuyama, Y., Yoshida, T., Tatsuoka, F., Koseki, J., Uchimura, T., Sato, N. & Oie, M. 2003. Shear banding characteristics of granular materials and particle size effects on the seismic stability of earth structures, *Proceedings of the 3rd International Symposium on Deformation Characteristics of Geomaterials, IS LYON 2003*, Vol. 2: 607-616: Balkema.

Tsutsumi, Y., Maqbool, S., Koseki, J. & Sato, T. 2006. Effects of large cyclic and creep loading on local deformation characteristics of compacted gravel, *Proceedings of the International Symposium on Mechanics and Geotechnics of Particulate Media*, Ube, Yamaguchi, Japan, September 12-14, 2006: 77-84: Balkema.

Tsutsumi, Y., Koseki, J. & Sato, T. 2008. Strain localization characteristics of dense Toyoura sand in plane strain compression tests under different confining pressures, *the 4th International Symposium on Deformation Characteristics of Geomaterials, IS Atlanta 2008*, Vol. 1: 365-370: Millpress.

Yoshida, T. & Tatsuoka, F. 1997. Deformation property of shear band in sand subjected to plane strain compression and its relation to particle characteristics, *Proceedings of the 14th International Conference on Soil Mechanics and Foundation Engineering*, Hamburg, 1: 237-240.